Tribol Lett (2014) 54:59–66
DOI 10.1007/s11249-014-0308-1

ORIGINAL PAPER

Gemini Interfaces in Aqueous Lubrication with Hydrogels

Alison C. Dunn · W. Gregory Sawyer · Thomas E. Angelini

Received: 22 November 2013 / Accepted: 13 February 2014 / Published online: 1 March 2014

Abstract The sliding interfaces found in the body—within the eyes, the digestive system, and the articulating joints, for example—are soft and permeable yet extremely robust, possessing low friction. The common elements among these systems are hydrophilic biopolymer networks that provide physical surfaces, elasticity, and fluid permeability. Stiff, impermeable probes are traditionally used to assess the frictional properties of most surfaces, including soft, permeable materials. However, both sides of physiological articulating interfaces are soft and hydrated. Measuring the friction response on just one-half of the cornea–eyelid interface or the cartilage–cartilage interface using a stiff, impermeable probe may not reproduce physiological lubrication. Here, we present lubricity measurements of the interface between two soft, hydrated, and permeable hydrogels. We explore the distinctions between the self-mated "Gemini" hydrogel interface and hydrogels sliding against hard impermeable countersurfaces. A rigid impermeable probe sliding against a soft permeable hydrogel exhibits strong frictional dependence on sliding speed, and a hydrogel probe sliding against flat glass shows a strong friction dependence on time in contact. The twin Gemini interface shows very low friction $\mu < 0.06$, with little dependence on sliding speed or time in contact. This consistently low-friction Gemini interface emulates the physiological condition of two like permeable surfaces in contact, providing excellent lubricity.

Keywords Hydrogel lubricity · Aqueous lubrication · Microtribology

1 Introduction

The human body possesses exquisite systems of lubrication that can withstand thousands of work cycles per day without fatigue. Lubrication of large articulating joints or the eyelid–cornea interface is critical to the health and function of their constituent tissues. The articular cartilage of the knee is composed of a highly structured network of collagen fibers, hyaluronin, and lubricin produced by encased chondrocyte cells [1–5]. Epithelial cells in the eye produce a protective and lubricating polymer network, the glycocalyx, which is composed of glycoprotein mucins, proteoglycans, and glycolipids (Fig. 1). Current understanding of weeping lubrication at the surfaces of these nanoporous biopolymer networks may be improved by exploring synthetic hydrogel friction; hydrogels with highly controlled stiffness, strength, water and ion permeability, and solubility allow for the isolation and systematic study of variables that control biological lubrication [6–10]. This versatility of hydrogels also facilitates experiments that explore the importance of self-mated surfaces; in both the eye and the knee, the sliding interface is composed of two near-identical, permeable, biological gels that hold water. Recent progress has been made in hydrogel friction studies that use hard, impermeable countersurfaces, yet the importance of the "twin" structure

A. C. Dunn · W. G. Sawyer (✉) · T. E. Angelini
Department of Mechanical and Aerospace Engineering, University of Florida, Gainesville, FL 32611, USA
e-mail: wgsawyer@ufl.edu

T. E. Angelini
J. Crayton Pruitt Family Department of Biomedical Engineering, University of Florida, Gainesville, FL 32611, USA

T. E. Angelini
Institute for Cell Engineering and Regenerative Medicine, University of Florida, Gainesville, FL 32611, USA

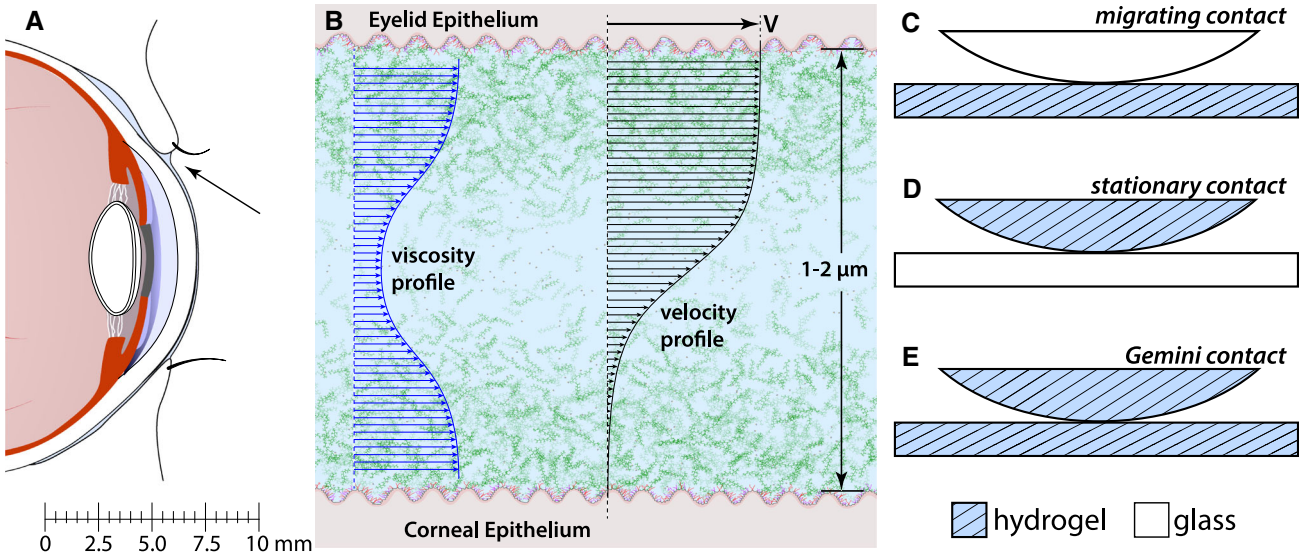

Fig. 1 **a** The eye is an exquisite system of lubrication comprising the epithelia and tear film. **b** The tear film composition is graded, with a higher concentration of mucins and glycoproteins near the epithelia. This schematic illustrates how the local sliding velocity between the eyelid and corneal epithelia drops off severely closer to the surfaces due to the high-viscosity mucinous gels. It is this system of self-mated hydrated gel lubrication that motivates this work using synthetic gels in aqueous lubrication. **c**–**e** Each contacting condition explored in the work is represented here as a schematic showing the hydrogel and glass components in the following order: migrating contact with glass probe and hydrogel flat; stationary contact with a hydrogel probe and glass flat; and self-mated, or Gemini contact, where both surfaces are hydrogel

of real biological lubricating interfaces has not been explored [11–16]. Pioneering work in biological lubrication utilized a self-mated interface that exhibited extremely low friction over a timescale of 10–20 min [17, 18]. Systematic studies of hydrogels that establish the role of twin surfaces in lubrication of soft, permeable materials will deepen our understanding of biological lubrication and broaden potential applications of hydrogels as surfaces engineered for lubricity.

Here, we study the effects of contact geometry and countersurface material on hydrogel lubricity. We explore three distinct types of contact: the migrating contact, in which a hemispherical glass probe slides across a flat hydrogel; the stationary contact, in which a hemispherical hydrogel probe slides across flat glass; and the self-mated contact, in which a hemispherical hydrogel probe slides against a flat hydrogel countersurface. We find that the coefficient of friction in the migrating contact geometry is strongly speed dependent, but only weakly time dependent. We observe the reverse behavior with the stationary contact geometry: the friction coefficient is strongly time dependent but weakly speed dependent. By contrast, the self-mated interface has very little dependence on sliding speed or on time. We interpret the behavior of migrating and stationary contact geometries, in which a hydrogel is pressed against a stiff, impermeable countersurface, with traditional concepts of lubrication. Lubrication of the self-mated contact, which exhibits an extremely low friction coefficient with no time or speed dependence, requires a new level of description because the traditional lubrication regimes do not manifest in this "Gemini" interface; there is no impermeable surface that can be supported by fluid pressure. This lubrication mechanism fundamentally differs from the fluid flow and lubrication of a hydrogel against an impermeable countersurface because the fluid flow and pressure are directed into a single side of the interface; these mechanisms lead to differences in observed friction depending upon the instrumental setup.

2 Materials and Sample Preparation

Polyacrylamide hydrogel samples were made by polymerizing acrylamide monomer (8 %), *N*,*N*′-Methylenebisacrylamide crosslinker (0.5 %), ammonium persulfate initiator (0.05 %), and tetramethylethylenediamine catalyst (0.15 %) in ultrapure water and an oxygen-deprived environment. All components are reported as mass-per-mass of solvent.

To create stationary, migrating, and self-mated configurations, we synthesized hemispherical probes and flat countersurfaces made from hydrogel, to be tested against one another or against glass. For the flat hydrogel surface, polyacrylamide was molded into a 1-mm-thick flat sheet between standard microscope slides, creating a smooth testing surface. A smooth frictional probe of known radius was made by polymerization in a two-part polyolefin mold, of which the hemispherical end was diamond turned to

achieve nanometer-scale roughness. The frictional probe geometry was designed to be a ~6-mm-long cylindrical shaft of radius 2.6 mm with a very smooth hemispherical end. The cylindrical portion was molded around a threaded rod for eventual fixation to the microtribometer flexure. After molding, the surface roughness of the probes was measured using scanning white light interferometry and found to be no more than 100 nm. Polymerized hydrogel samples of both geometries were equilibrated in ultrapure water for 24 h before experiments began, and no swelling or shrinking occurred.

3 Experimental Methods

3.1 Tribometer Configuration and Measurement Setup

Friction experiments were run on a custom microtribometer, with low-force capabilities in the micronewton range, as described in previous work [14, 19]. In this case, the vertical piezoelectric stage used to translate down and apply the normal force had a range of 1,500 μm. The reciprocating stage was exchanged from a piezoelectric stage to a servo-motor linear stage (Physik Instrumente, Auburn, MA) in order to achieve a longer free-sliding distance of 3 mm of travel between reversals.

The following process was used in order to measure lubricity during free sliding between the hydrogel samples and various countersurfaces. First, the probe and flat were mounted into the instrument in close proximity and hydrated by the addition of approximately 500 μL of ultrapure water. The frictional probe was slowly lowered until contact was detected; contact was distinguished from background noise and capillary force variations by a monotonic increase in force up to 100 μN. The probe was retracted to a few micrometers from contact, and the forces were zeroed to minimize capillary force changes due to vertical probe displacement during approach. After setup, the experiment was run by lowering the piezoelectric stage and frictional probe until the desired applied normal force was reached, the reciprocating the lateral stage over a prescribed number of cycles, measuring the friction force.

3.2 Experiments

In order to interrogate differences between stationary, migrating, and self-mated contact conditions in hydrogel lubrication, three distinct experimental setups were assessed. Migrating contact was provided by placing the flat sheet of polyacrylamide hydrogel on the reciprocating stage and by sliding it with respect to a polished sapphire probe at a given applied normal force (Fig. 1c). The normal force in this case was chosen to be 400 μN in order to apply pressures that typically exist between the eyelid and cornea/sclera in normal physiological function (1–6 kPa) [20]. Stationary contact was provided by replacing the polished sapphire probe with the polyacrylamide hydrogel probe and by replacing the flat sheet with a simple microscope slide (Fig. 1d). The sapphire and glass components were cleaned before each experiment using isopropanol on a fiber-free wipe. Self-mated "Gemini" contact was achieved by combining these setups to include both the hydrogel flat sheet and the soft probe (Fig. 1e).

The hydrogel compression under an applied load of 400 μN should be unaffected by substrate support due to the thickness of the hydrogel both in the flat sheet and at the apex of the probe. A Hertzian approximation of the maximum deformation of the flat sheet under a glass probe using an elastic modulus of ~50 kPa gives only 20 μm, approximately 2 % of the hydrogel thickness. The corresponding upper limit on the contact width is less than the hydrogel slab thickness, further reducing the potential role of the glass substrate. The shallow indentation depth of this work differentiates it from studies of hydrated polymer brushes. Substrate effects in this work are neglected, while in polymer brush friction studies, they dominate the pressure profile and force water from the brushes under high pressures up to 20 MPa [21].

The range of speeds explored in these experiments was chosen to be on the order of 100's of μm/s, which is relevant to a wide range of biological lubricating interfaces. We incrementally varied the sliding speed over these values: 100, 200, 300, 400, 500, 800, and 1,500 μm/s. Each experiment was run for 30 reciprocating sliding cycles over a 3-mm stroke length; for the slowest speed of 100 μm/s, the experiment lasted 30 min, and for the fastest speed of 1,500 μm/s, the experiment lasted only 2 min. Data were acquired at ~530 Hz, so more than 400 data points were used to calculate the friction coefficient during a single reciprocating cycle, even at the fastest sliding speeds. These data were analyzed for the local friction response along the sliding location on the hydrogel or glass and then for the average friction coefficient in each of the 30 cycles. The reported friction coefficients were calculated by averaging the ratio of the friction force over the normal force in the middle 20 % of the free-sliding region for each reciprocating cycle.

4 Results

4.1 Initiation of Sliding After Dwell

Friction traces map out the friction coefficient in space and time as the probe slides in forward and reverse directions through a single reciprocation cycle (Fig. 2a–c). With a

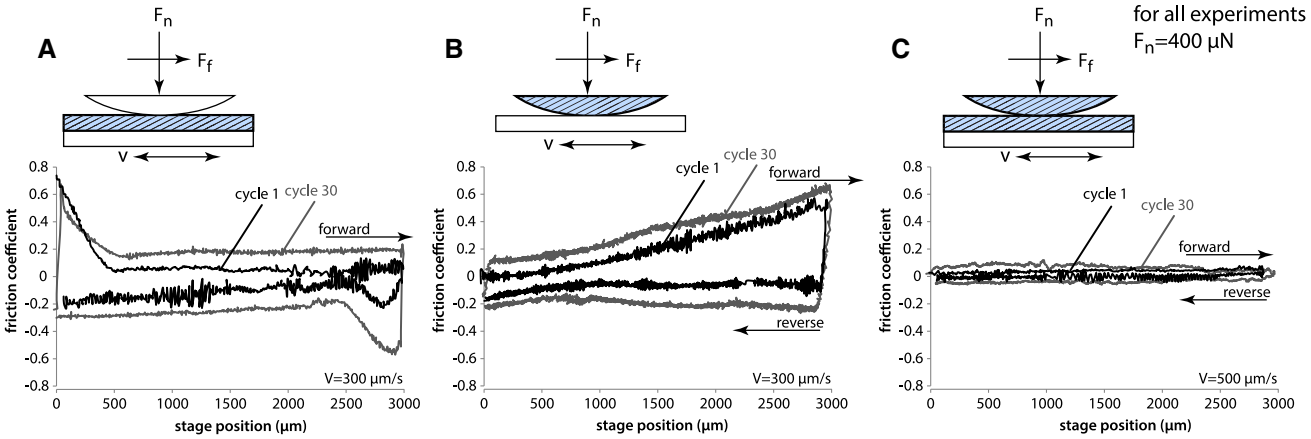

Fig. 2 The friction traces for each contact setup are distinct. **a** Migrating contact friction traces leave each reversal with a large breakloose force followed by smooth sliding between the reversals. **b** Stationary contact does not indicate location-specific friction and lacks a distinct breakloose region. The higher friction coefficient at the rightmost stage positions arises from slight reciprocating stage misalignment with respect to the vertical axis of load application. **c** Self-mated contact shown on the same scale has a friction coefficient low enough that no features are easily discernible

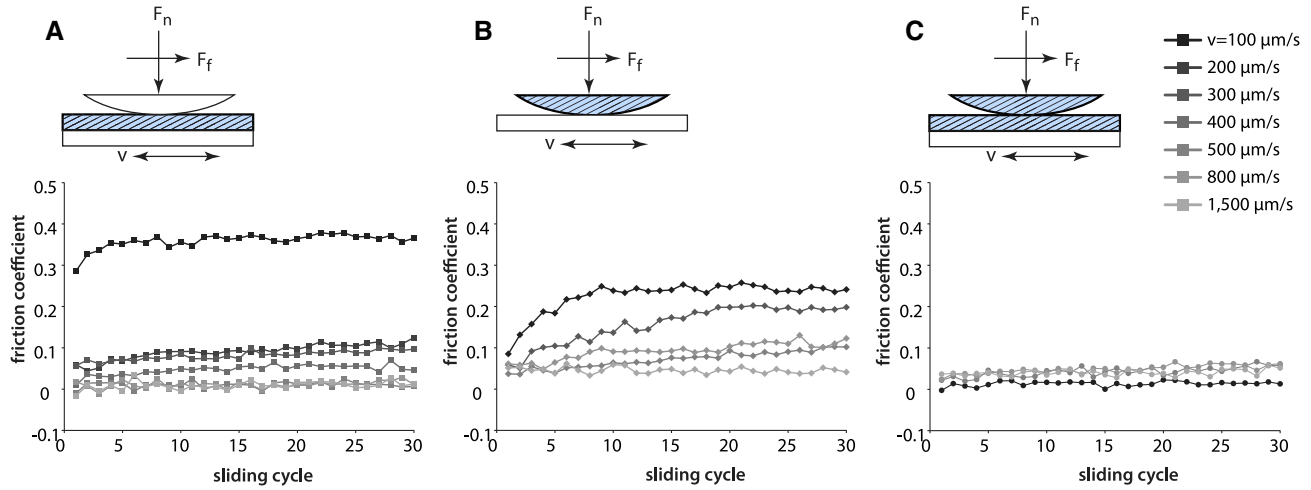

Fig. 3 Friction coefficient over 30 consecutive sliding cycles for all contact conditions, plotted on a linear scale. **a** In the migrating condition, friction coefficient continues to decrease to measurement limits. **b** Stationary contact does not reach the same low friction at the highest sliding speeds of >1,000 μm/s. Migrating and stationary contact conditions exhibit strong speed- and time-dependent friction coefficient, respectively. **c** In the self-mated condition, friction remains low, $\mu < 0.06$, for all sliding speeds over all times

migrating contact, as the translation stage begins to move following a turnaround point, the glass probe breaks free from a short dwell against the flat hydrogel sample. The friction trace for cycles 1 and 30 in migrating contact shows a distinct peak in breakloose friction coefficient, $\mu = 0.7$, followed by a much lower free-sliding friction coefficient: $\mu = 0.2$ and $\mu = 0.1$ for cycles 1 and 30, respectively. In contrast, the friction trace for stationary contact shows no breakloose features because the same location on the hydrogel sample is continuously in contact with glass. Though the surface was very smooth over the 3 mm of sliding, the microscope slide countersurface was misaligned very slightly to the vertical axis of force measurement, which is manifested in the right side of the friction loop being wider. The additive effect of normal force into the friction force causes this orientation-dependent hysteresis. However, the average normal forces and friction forces are calculated from the middle 20 % of the stage position for every cycle, where the average applied normal force is kept at 400 μN. The Gemini interface friction loops exhibit a uniformly low friction coefficient over all trace locations including reversal regions. The different characters of these friction loops are the first indications that the three types of interfaces studied here are qualitatively different. The friction coefficients extracted from friction loops, for all cycles and all sliding speeds, are shown in Fig. 3.

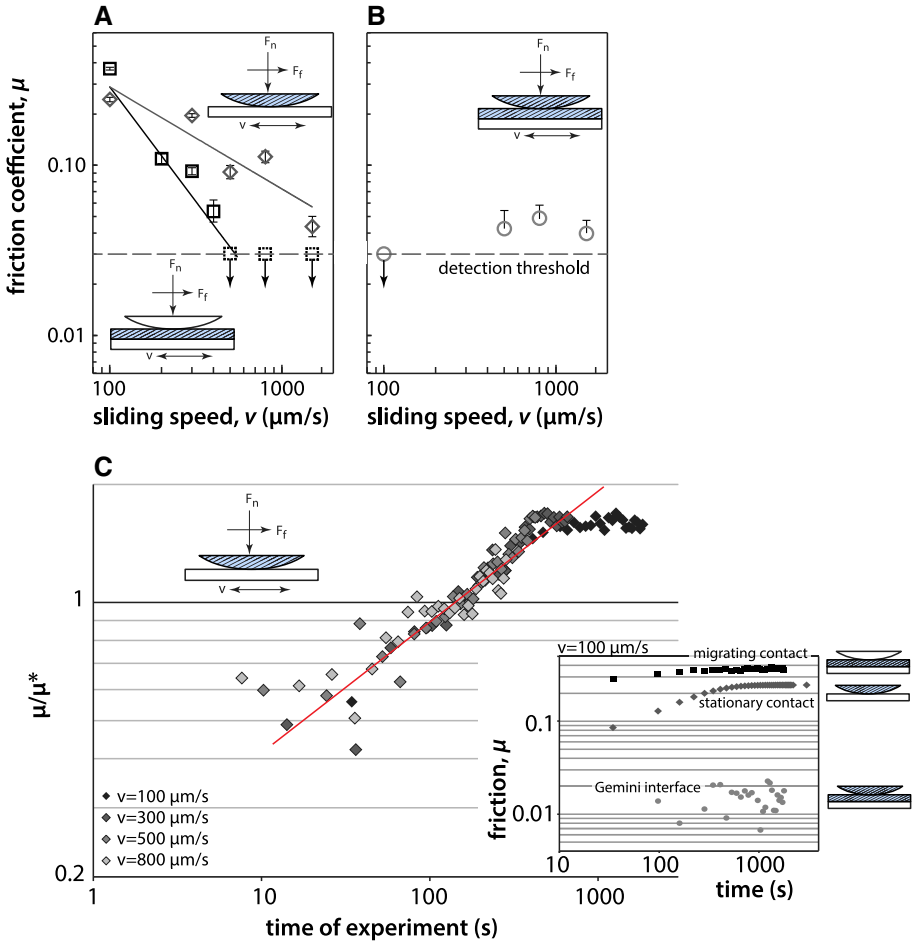

Fig. 4 **a** The migrating and stationary contacting conditions are both sensitive to sliding speed, with the migrating condition exhibiting more sensitivity. For an applied load of $F_n = 400$ μN, the friction coefficient in migrating contact drops three times faster than that of stationary contact for the same sliding speeds. **b** The sensitivity of these experiments is $\mu = 0.03$, indicated by the *dashed line*. Measurements below this threshold are shown on the *line*. Within uncertainty estimates, the friction coefficient for self-mated "Gemini" contact does not have a discernible slope. **c** The friction coefficients from the stationary contacting condition collapse to a single scaling law with an exponent of 1/3. *Inset plot* shows friction versus time for all setups at a sliding speed of 100 μm/s and differentiates the time-dependent character of the stationary contact contrasted with the other two conditions

4.2 Strong Speed Dependence in Migrating Contact Friction

The increased breakloose friction observed following reversals with the migrating contact interface suggests that sliding speed affects friction more in migrating contact geometries than in stationary or Gemini contacts. At the slowest sliding speed of 100 μm/s in the migrating contact condition, the friction coefficient was highest, at $\mu = 0.366 \pm 0.030$, and as the sliding speed was increased, the friction coefficient decreased down to very low values of $\mu < 0.02$, though the noise introduced by the motorized stage caused the uncertainty to increase. Overall, the decrease in friction coefficient was significant (Fig. 3a). In stationary contact conditions, the friction coefficient also decreases with increasing sliding speed, but with a much weaker dependence, spanning a range of $\mu = 0.043 \pm 0.060$ to 0.241 ± 0.020. In Gemini contact conditions, the friction exhibits no significant speed dependence, staying low at $\mu = 0.015 \pm 0.020$ to 0.058 ± 0.080 (Fig. 3b, c). To further differentiate these three types of contact, we explore the scaling of μ versus sliding speed, v. At each sliding speed, we compute an average coefficient of friction, taken over the last ten cycles where transient behavior has died out. Plotting this average, long-time friction coefficient versus sliding speed on a log–log scale, we find that μ scales approximately like $v^{-1/2}$ in the stationary contacting condition. The migrating contact is dramatically more sensitive to sliding speed, with μ scaling like $v^{-3/2}$ (Fig. 4a). The Gemini contact differs from both other contacting conditions, with μ exhibiting no speed dependence at all within measured uncertainties.

4.3 Strong Time Dependence in Stationary Contact Friction

The friction coefficient in the stationary contacting condition rises slowly and monotonically with increasing cycle number for constant applied normal force and for all sliding speeds up to 800 μm/s (Fig. 3b). At a single sliding speed, the friction coefficient can vary approximately by a factor of 4, from 0.05 to 0.2, at $v = 300$ mm/s for example. When plotted versus time on a log–log scale, μ appears to rise like a weak power law at intermediate times for all sliding speeds, which results in the collapse of all data when each curve is rescaled by its own friction coefficient at any single time between 1 and 5 min. This collapse

suggests that all curves follow the same scaling law, $\mu = At^{p}$. The high degree of uncertainty in fitting a weak power law over only two decades in t and one decade in μ prohibits a confident determination of p; however, the data appear to scale like $t^{1/3}$ (Fig. 4c). In the cases of migrating and Gemini contacts, by contrast, the friction coefficient measured with increasing cycle number and time shows almost no time dependence at all (Figs. 3a, d, 4c, inset).

The scaling of μ with time to the 1/3 power can be predicted with a minimal back-of-the-envelope model of the stationary contact geometry. The hydrogel described here has an extremely low Young's modulus of 30 kPa, so we expect that the gel's slow response to the applied normal load is dominated by the viscous drag forces required to push fluid through the polymer probe while it compresses against the glass countersurface. The time dependence of this process is described by Darcy's law, $Q = k_{\text{eff}} \Delta P$, where $Q = \mathrm{d}V/\mathrm{d}t$ is the volumetric flow rate through material with effective permeability k_{eff}, and ΔP is the driving pressure drop across the material. The hemispherical hydrogel probe tip is flattened over time during stationary sliding, and the amount of volume displaced from the equivalent hemispherical cap can be written as a function of flat contact area, $V = (4\pi R)^{-1}A^2$, where R is un-deformed probe radius of curvature, and the small-angle approximation is assumed. We equate the time derivative of this volume to Q, allowing Darcy's law to be recast in terms of contact area, $2A(\mathrm{d}A/\mathrm{d}t)(4\pi R)^{-1} = k_{\text{eff}} F_n/A$, where the normal force divided by the contact area, F_n/A, is the driving pressure ΔP. The approximation $F_n/A \approx \Delta P$ is valid for the hydrogel used here, in which the Biot–Willis coefficient is approximately 1, and the elastic stress is much less than the applied pressure throughout most of the indentation process [22]. Simplifying, we are left with a differential equation that describes how the soft, permeable probe contact area increases with time in stationary contact, $\mathrm{d}A/\mathrm{d}t = CA^{-2}$, where C contains all of the geometric factors, the material permeability, and the normal force. The resulting contact area, $A(t) = (3Ct)^{1/3}$, has the same scaling with time as the measured friction coefficient; for soft materials in conformal contact, the friction coefficient is proportional to the interfacial contact area. This simple prediction can be greatly improved using more sophisticated models of the probe and accounting for the changes in k_{eff} over time.

5 Discussion

Each of the three interfaces described here is lubricated by water, dominantly by a different mechanism. All three involve a soft permeable hydrogel and conformal contact between two surfaces. A flat hydrogel slab sliding against a hemispherical glass probe experiences local, periodic, applied loads; the contact spot constantly moves along the hydrogel. In this migrating contact configuration, we find that friction coefficient depends strongly on sliding speed and that the glass probe indents the gel more at the reversals where sliding speed briefly drops to zero. These observations suggest that friction in a migrating contact is controlled by a balance of two rates: the rate at which the glass probe indents the permeable hydrogel and the rate at which the probe slides to an un-indented region. This balance sets a steady-state indentation depth in the gel that moves locally with the probe. Faster sliding results in less indentation into the hydrogel, a lower contact area, and a smaller measured friction force.

A hemispherical hydrogel sliding against flat glass is an under-persistent load. The contact spot moves along the glass, but remains in the one place on the gel. In this stationary contact, we find that friction coefficient depends only weakly on speed, but strongly on time under applied load, with a time constant of order 100 s. This order of magnitude can be predicted by calculating the hydrogel permeability, $k = \xi^2/\eta$, where ξ is network the mesh size and η is the viscosity of water [23]. The mesh size, ξ, of polyacrylamide at the concentrations used here is $\sim$20 nm [24], yielding a permeability of $k = 0.4\ \text{mm}^4\ \text{N}^{-1}\ \text{s}^{-1}$. Using this permeability in Darcy's law, $V/\tau = AkL^{-1}\Delta P$, where V is the volume displaced over time, τ, through an effective cross-section, A, over a distance, L, we make an order-of-magnitude estimate of the time to displace the volume of a hemispherical cap. Approximating A as the surface area of a cylinder with a diameter equal to the contact width, a, and height equal to the indentation depth, we find a simple relationship for the timescale, $\tau \sim a^4 k^{-1} F_n^{-1}$, where the probe radius and the indentation depth drop out of the problem. For our experimental parameters, we predict τ of order 100 s. Our findings therefore suggest that hydrogel permeability and applied load dictate an equilibration rate of approach to steady-state friction coefficient in stationary contacts.

A hemispherical hydrogel probe sliding against a flat hydrogel slab is a combined condition where the probe retains a stationary contact area and the slab experiences a migrating contact area, simultaneously. In this matched Gemini interface, the friction coefficient never rises above $\mu = 0.058$ for any time point at any sliding speed; within the measurement uncertainty, the friction coefficient is the same. This result does not appear to be a superposition of the individual corresponding asymmetric contact responses because we see neither speed dependence nor time dependence of the friction coefficient. The lubrication of both stationary and migrating interfaces is controlled by the response of the hydrogel side of the contact, yet combining two hydrogels into a Gemini interface does not merely

reduce the speed or time dependence of friction by a factor of two. Rather, the speed and time dependence vanishes completely. This qualitative difference can be understood from the potential interactions that occur at the three kinds of interface. In the stationary and migrating contacts, the glass side of the interface provides a continuous surface for generating polymer–glass interactions. By contrast, both sides of the hydrogel Gemini interface are mostly water, reducing the probability of chain–chain interactions by orders of magnitude. Moreover, the polymers on both sides of the Gemini interface are solvated, further reducing chain–chain interactions, similar in spirit to hydration lubrication observed in polymer brush monolayers [21].

In both the stationary contact and the stationary half of the Gemini hydrogel interface, the ultimate degree of compression is controlled by the network elasticity and the applied load. The combination of hydrogel permeability, elasticity, and applied load dictates an equilibration time required to reach a steady-state friction coefficient. The intimate connection between hydrogel permeability and elasticity, through their strong dependence on network mesh size, will produce widely varying equilibration times and ultimate friction coefficients for hydrogels of differing composition, possibly even in the presence of boundary lubricants. In our order-of-magnitude estimates above, the radius of curvature and indentation depth drop out of the problem, allowing the estimate to be extended other systems like articular cartilage. Cartilage has about 1/100th the permeability of the polyacrylamide hydrogel used here and a comparable elastic modulus; our equilibration time estimate predicts τ on the order of hours for cartilage. Thus, long periods of pressure on joints, even with no motion, do not result in significantly high startup friction. These long timescales meet the requirements of fluid load support, in which the relaxation rate of a poroelastic material competes with sliding speed [2, 25]. In the Gemini hydrogel interface, however, there is no impermeable surface to be supported by the fluid, and the details of the resulting lubrication mechanism remain to be revealed.

Lubrication in traditional engineering is well captured by the Stribeck curve that emerges from the log–log plotting of the friction coefficient versus a dimensionless bearing number such as ($\eta V/F_n'$). This x-axis can also be nearly equivalently represented as a dimensionless ratio of the film thickness to a combined surface roughness of the pair. For films that are on the order of the surface roughness, boundary lubrication describes the physical contacting of the hard asperities during sliding, and the friction coefficients are correspondingly high with characteristic values above $\mu = 0.1$. In contrast, our studies on the lubrication that occurs at the interface between hydrogels under conditions of vanishingly thin (negligible) hydrodynamic films suggest that the contact contains significant interfacial water and that the area of contact is set by both the permeability and the elastic modulus. In hydrogels, both the permeability and the elastic modulus are dominantly controlled by the hydrogel network mesh size. The mesh size determines the rate at which water can be pushed through the network under a given pressure gradient and defines the elasticity of the gel. The critical role of the polymer mesh size in controlling the Gemini hydrogel interface leads us to call this mode of lubrication *mesh-confined lubrication*.

In engineering systems, rather abrupt transitions occur over narrow ranges in fluid film thickness. Typical engineering surfaces have elastic moduli of gigapascals and greater and have roughnesses well below 1 μm, often in the range of 10's of nanometers. Thus, as hydrodynamic fluid films begin to become established, there is transition region over which the sliding interface goes from contacting to separated. In stark contrast, these soft hydrogel surfaces are completely deformed into conformal contact and contain interfacial water films even in the absence of hydrodynamics. Because of the mesh-confined action of these Gemini hydrogel interfaces, motion further creates an interface that is increasingly hydrated. Moreover, both natural and synthetic hydrogels are covered with extended

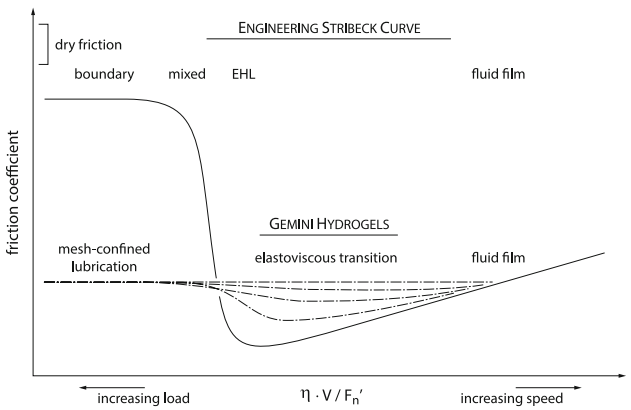

Fig. 5 A schematic illustration of an engineering *Stribeck curve* is shown above with traditional modes of lubrication roughly indicated: dry friction, boundary lubrication, elastohydrodyamic lubrication (EHL), and fluid film lubrication. Impermeability of the interfaces is inherent in the formulation of the classical fluid mechanics theories from which the modes of lubrication were named (e.g., EHL and fluid film). Gemini hydrogel lubrication builds from a conceptual framework of matched permeable surfaces that may involve fluid transport both across and along the "contacting" interface. At slow speeds or high loads, the mechanism of lubrication is thought to be attributable to the role of the hydrogel mesh size acting to confine and preserve fluid within the contact. At high speeds or low loads, the act of hydrodynamic lubrication is only weakly affected by having permeable interfaces. Between the regions of mesh-confined lubrication and fluid film lubrication, we anticipate an elastoviscous transition in which the most extended polymer chains interact with the fluid to effectively create a dynamic shear and pressure dependent viscosity across the interface

polymer chains that we suspect begin to influence the interfacial viscosity through elastoviscous action that is dictated by the surface separation lengths. As these Gemini hydrogel surfaces begin to separate, the decreasing effective viscosity with increasing fluid separation, occurring in concert with an increasing shear rate, has a net smoothing effect that damps frictional transitions between contact and fluid film lubrication. This postulated *elastoviscous transition* is illustrated in Fig. 5, which schematically contrasts the lubrication behavior of Gemini hydrogel interfaces to the classic engineering Stribeck curve.

Gemini hydrogel interfaces are likely ubiquitous in healthy low-friction biological interfaces such as articular cartilage, proteinaceous connective tissues, mucin-covered surfaces and tissues, and the glycocalyx and glycoproteins of the cellular epithelium. We anticipate that matching permeability and mechanics through the careful design of both hydrogel mesh size and component geometry will emerge as critical parameters in determining the successes or failures of hydrogels as biological replacement tissues or tissue mimics. Recent reports of hydrogel lubricity that employed asymmetric contact testing conditions [15] may be subject to effects that were found to be dominant in our study. Perhaps the greatest opportunity for breakthroughs in this area is in developing a deep theoretical understanding of the postulated elastoviscous transition region, and developing materials and surfaces that are capable of producing a nearly constant low-friction interface across all ranges of speeds and loads.

Acknowledgments The authors gratefully acknowledge Professor Duncan Dowson and Professor Nic Spencer for patient and scholarly discussions. Additionally, we are indebted to Professor Philippa Cann and Dr. Connor Myant for their thoughts on aqueous lubrication. This work was funded by Alcon Laboratories, and we thank Mr. Allen Gilliard for fabricating the hydrogel probe polyolefin molds.

References

1. Ateshian, G.A.: The role of interstitial fluid pressurization in articular cartilage lubrication. J. Biomech. **42**(9), 1163–1176 (2009). doi:10.1016/j.jbiomech.2009.04.040
2. Ateshian, G.A., Wang, H.: Rolling resistance of articular cartilage due to interstitial fluid flow. Proc. Inst. Mech. Eng. H: J. Eng. Med. **211**(5), 419–424 (1997). doi:10.1243/0954411971534548
3. Brown, S.S., Clarke, I.C.: A review of lubrication conditions for wear simulation in artificial hip replacements. Tribol. Trans. **49**(1), 72–78 (2006). doi:10.1080/05698190500519223
4. Glasson, S.S., Askew, R., Sheppard, B., Carito, B., Blanchet, T., Ma, H.L., Flannery, C.R., Peluso, D., Kanki, K., Yang, Z.Y., Majumdar, M.K., Morris, E.A.: Deletion of active ADAMTS5 prevents cartilage degradation in a murine model of osteoarthritis. Nature **434**(7033), 644–648 (2005). doi:10.1038/Nature03369
5. Schmidt, T.A., Sah, R.L.: Effect of synovial fluid on boundary lubrication of articular cartilage. Osteoarthr. Cartil. **15**(1), 35–47 (2007). doi:10.1016/j.joca.2006.06.005
6. Jen, A.C., Wake, M.C., Mikos, A.G.: Review: hydrogels for cell immobilization. Biotechnol. Bioeng. **50**(4), 357–364 (1996). doi:10.1002/(Sici)1097-0290(19960520)50:4<357:Aid-Bit2>3.0.Co;2-K
7. Kirschner, C.M., Anseth, K.S.: Hydrogels in healthcare: from static to dynamic material microenvironments. Acta Mater. **61**(3), 931–944 (2013). doi:10.1016/j.actamat.2012.10.037
8. Mathur, A.M., Moorjani, S.K., Scranton, A.B.: Methods for synthesis of hydrogel networks: a review. J. Macromol. Sci. **36**(2), 405–430 (1996)
9. Richter, A., Paschew, G., Klatt, S., Lienig, J., Arndt, K.F., Adler, H.J.P.: Review on hydrogel-based pH sensors and microsensors. Sensors **8**(1), 561–581 (2008). doi:10.3390/S8010561
10. Sun, J.Y., Zhao, X.H., Illeperuma, W.R.K., Chaudhuri, O., Oh, K.H., Mooney, D.J., Vlassak, J.J., Suo, Z.G.: Highly stretchable and tough hydrogels. Nature **489**(7414), 133–136 (2012). doi:10.1038/Nature11409
11. Bonnevie, E.D., Baro, V.J., Wang, L., Burris, D.L.: Fluid load support during localized indentation of cartilage with a spherical probe. J. Biomech. **45**(6), 1036–1041 (2012). doi:10.1016/j.jbiomech.2011.12.019
12. Gleghorn, J.P., Bonassar, L.J.: Lubrication mode analysis of articular cartilage using Stribeck surfaces. J. Biomech. **41**(9), 1910–1918 (2008). doi:10.1016/j.jbiomech.2008.03.043
13. Krishnan, R., Kopacz, M., Ateshian, G.A.: Experimental verification of the role of interstitial fluid pressurization in cartilage lubrication. J. Orthop. Res. **22**(3), 565–570 (2004). doi:10.1016/j.orthres.2003.07.002
14. Rennie, A.C., Dickrell, P.L., Sawyer, W.G.: Friction coefficient of soft contact lenses: measurements and modeling. Tribol. Lett. **18**(4), 499–504 (2005). doi:10.1007/s11249-005-3610-0
15. Roba, M., Duncan, E.G., Hill, G.A., Spencer, N.D., Tosatti, S.G.P.: Friction measurements on contact lenses in their operating environment. Tribol. Lett. **44**(3), 387–397 (2011). doi:10.1007/s11249-011-9856-9
16. Zhou, B., Li, Y.T., Randall, N.X., Li, L.: A study of the frictional properties of senofilcon-A contact lenses. J. Mech. Behav. Biomed. Mater. **4**(7), 1336–1342 (2011). doi:10.1016/j.jmbbm.2011.05.002
17. Lewis, P.R., Mccutchen, C.W.: Experimental evidence for weeping lubrication in mammalian joints. Nature **184**(4695), 1285 (1959). doi:10.1038/1841285a0
18. Mccutchen, C.W.: Sponge-hydrostatic and weeping bearings. Nature **184**(4695), 1284–1285 (1959). doi:10.1038/1841284a0
19. Krick, B.A., Vail, J.R., Persson, B.N.J., Sawyer, W.G.: Optical In situ micro tribometer for analysis of real contact area for contact mechanics, adhesion, and sliding experiments. Tribol. Lett. **45**(1), 185–194 (2012). doi:10.1007/s11249-011-9870-y
20. Shaw, A.J., Collins, M.J., Davis, B.A., Carney, L.G.: Eyelid pressure and contact with the ocular surface. Invest. Ophthalmol. Vis. Sci. **51**(4), 1911–1917 (2010). doi:10.1167/Iovs.09-4090
21. Gaisinskaya, A., Ma, L.R., Silbert, G., Sorkin, R., Tairy, O., Goldberg, R., Kampf, N., Klein, J.: Hydration lubrication: exploring a new paradigm. Faraday Discuss. **156**, 217–233 (2012). doi:10.1039/C2fd00127f
22. Wang, H.F.: Theory of Linear Poroelasticity with Applications to Geomechanics and Hydrogeology. Princeton University Press, Princeton (2000)
23. DeGennes, P.-G.: Scaling Concepts in Polymer Physics. Cornell University Press, Ithaca (1979)
24. Hsu, T.P., Cohen, C.: Observations on the structure of a polyacrylamide-gel from electron-micrographs. Polymer **25**(10), 1419–1423 (1984). doi:10.1016/0032-3861(84)90103-4
25. Moore, A.C., Burris, D.L.: An analytical model to predict interstitial lubrication of cartilage in migrating contact areas. J. Biomech. **47**, 148–153 (2014). doi:j.jbiomech.2013.09.020